Néel temperature and magnetic phase boundary of the spin-$\frac{1}{2}$ Heisenberg antiferromagnet in three dimensions

Kok-Kwei Pan
Physics Group, Center of General Education, Chang Gung University, No. 259, Wen-Hua 1st Road, Kwei-San, Tao-Yuan, Taiwan, Republic of China
(Received 24 August 1998)

We obtained the eighth-order linked-cluster series for the free energy, the sublattice magnetization, and the staggered susceptibility of the spin-$\frac{1}{2}$ Heisenberg antiferromagnet on three-dimensional bipartite lattices. The series are analyzed using the standard extrapolation techniques with the application of a conformal transformation method to obtain the Néel temperature and the temperature dependence of sublattice magnetization. We obtain a more accurate estimate of the Néel temperature and the magnetic phase boundary for the body-centered cubic and the simple cubic lattices. The results are compared with related works.
[S0163-1829(99)09601-0]

I. INTRODUCTION

The Heisenberg antiferromagnetic model has received considerable interest in recent years because of the wide variety of critical phenomena exhibited in this system. This model has also attracted much attention recently because of its possible relevance to the phenomenon of high-temperature superconductivity. The thermodynamic properties and the phase transition of this model in three dimensions have been investigated by a variety of approximate methods which include spin-wave theory,[1,2] high-density expansion,[3] the high-temperature series expansion method,[4] the Green function method,[5] and the variational cumulant expansion.[6] Despite these efforts the detailed analysis of the critical point and thermodynamic behavior of three-dimensional Heisenberg antiferromagnetic model are not known. The low-temperature behavior is better described by spin-wave theory. At temperatures above the transition point, the high-temperature series expansion method has been used to obtain an estimate of the Néel temperature.

In this paper we study the phase transition and the magnetic phase boundary of the spin-$\frac{1}{2}$ quantum Heisenberg antiferromagnet using the linked cluster series expansion method. The linked cluster series expansion method has provided the most accurate results in the study of phase transition and critical phenomena in spin systems.[7] This method has been extensively used on ferromagnetic spin systems.[8] The method sums up all perturbation terms to a certain order and estimates the result through a well-developed extrapolation method. The accurate results are obtained both in the ordered phase and disordered phase. In the disordered phase the linked cluster series are identical to the high-temperature series.

We have obtained the exact eighth-order linked-cluster series for the free energy, sublattice magnetization, and staggered susceptibility of the spin-$\frac{1}{2}$ Heisenberg antiferromagnet in an external magnetic field[9] on three-dimensional bipartite lattices. In the present work we study the thermodynamic properties of the model in zero external magnetic field. In the disordered phase our staggered susceptibility series reduces to that of high-temperature series expansion with an addition of two terms to the previous work.[4] In the ordered phase, correlations of spin and thermal fluctuations are included in the perturbation expansion and the order parameter is found self-consistently from the series of the sublattice magnetization. The series are analyzed using standard extrapolation techniques[10] with the application of a conformal transformation method to obtain a more accurate estimate of the Néel temperature and the temperature dependence of sublattice magnetization.

A brief outline of the paper is as follows. In Sec. II we discuss the linked-cluster series expansion method applied to the spin-$\frac{1}{2}$ Heisenberg antiferromagnetic model. The results of the calculations are presented in Sec. III. A comparison with related works is also presented. A summary and conclusions is given in Sec. IV.

II. DERIVATION OF THE SERIES

The Hamiltonian of the spin-$\frac{1}{2}$ Heisenberg antiferromagnet is given as

$$H=\sum_{\langle i,j\rangle} J_{ij}\mathbf{S}_i\cdot\mathbf{S}_j-h_A\sum_{i\in A} S_i^z-h_B\sum_{j\in B} S_j^z, \tag{1}$$

where i and j refer to the sites of two distinct interpenetrating sublattice and the pair interaction parameter $J_{i,j}$ is taken to be $J>0$ when i and j are nearest neighbors and zero otherwise. h_A and h_B in the Zeeman energy term are staggered magnetic fields on two sublattice A and B for calculating the sublattice magnetization and staggered susceptibility. We have divided the lattice sites into two distinct interpenetrating sublattices.

The Hamiltonian is divided into an unperturbed Hamiltonian H_0 and a perturbation part as H_1

$$H=H_0+H_1. \tag{2}$$

H_0 includes all single-ion potentials and a self-consistent field term extracted from the two-ion interaction potential.

The self-consistent field is characterized by two parameters $M_A=\langle S_A^z\rangle$ and $M_B=\langle S_B^z\rangle$ which minimize the free energy of the system:

$$H_0=\sum_{i\in A}[JzM_B-h_A]S_i^z+\sum_{j\in B}[JzM_A-h_B]S_j^z - \frac{1}{2}NJzM_AM_B, \tag{3}$$

where z is the number of nearest neighbors and N is the total number of sites in a lattice.

H_1 includes the effects of correlations of the fluctuations:

$$H_1=J\sum_{\langle i,j\rangle}[S_i^z-M_A][S_j^z-M_B]+\frac{J}{2}\sum_{\langle i,j\rangle}[S_i^+S_j^-+S_i^-S_j^+]. \tag{4}$$

The eigenstates for the local site of H_0 are $|1\rangle=|\uparrow\rangle$ and $|\overline{1}\rangle=|\downarrow\rangle$ and the corresponding eigenenergies for sublattice A and B are

$$\epsilon_1^A=\frac{1}{2}\{JzM_B-h_A\},\quad \epsilon_1^B=\frac{1}{2}\{JzM_A-h_B\}, \tag{5}$$

$$\epsilon_{\overline{1}}^A=-\frac{1}{2}\{JzM_B-h_A\},\quad \epsilon_{\overline{1}}^B=-\frac{1}{2}\{JzM_A-h_B\}, \tag{6}$$

apart from the constant energy from $-\frac{1}{2}JzM_AM_B$. We consider the symmetrical case of equal and opposite staggered field, $h_A=-h_B=h_s(h_s>0)$. In this case $M_A=-M_B=M^+(M^+>0)$. The mean-field free energy per site F_0 is

$$F_0=-\frac{1}{\beta}\left\{\ln\left[2\cosh\left(\frac{1}{2}y\right)\right]\right\}, \tag{7}$$

where $y=\beta\{JzM_0^++h_s\}$.

The mean-field sublattice magnetization per site M_0^+ is obtained from the free energy by taking a derivative with respect to h_s,

$$M_0^+=-\frac{\partial F_0}{\partial h_s}=\frac{1}{2}\tanh\left(\frac{1}{2}y\right). \tag{8}$$

The corrections of free energy to F_0 due to the quantum and thermal fluctuation correlations is expressed as[11] a sum over all connected diagrams:

$$\Delta F=-\frac{1}{\beta}\sum_{n=1}^{\infty}\frac{(-1)^n}{n!}\int_0^\beta d\tau_1\int_0^\beta d\tau_2\cdots \times\int_0^\beta d\tau_n\langle T_\tau[H_1(\tau_1)H_1(\tau_2)\cdots H_1(\tau_n)]\rangle_c, \tag{9}$$

where $\beta=(k_BT)^{-1}$.

The terms in the series expansion are often written as a sum over all connected diagrams which are composed of spin operators:

$$\Delta F=\sum_{n,g_n}^{\infty}W(g_n)L(g_n)I(g_n). \tag{10}$$

TABLE I. Exact coefficients of the staggered susceptibility series of the spin-1/2 Heisenberg antiferromagnet model in the disordered phase for the bcc and sc lattices.

a_n	bcc	sc
a_0	0.25	0.25
a_1	0.50	0.375
a_2	0.833333	0.4375
a_3	1.333333	0.46875
a_4	2.024479	0.483203
a_5	3.024392	0.501367
a_6	4.454776	0.512950
a_7	6.515440	0.512135
a_8	9.455114	0.505525

The summation is over all linked graphs where g_n indicates an nth-order linked graph. $W(g_n)$ is the weight of the graph or the number of topologically equivalent graphs appear in the expansion. $L(g_n)$ is the *lattice constant* of the graph. $I(g_n)$ is the value of the nth-order τ integral of the cumulant product which the graph represents. The connected graphs and the weights of the graphs are produced from the Ising graphs by an algorithm which has been implemented on a computer. For example, for the simple cubic and body-centered cubic lattices, there are 43 distinct graphs for sixth order, 82 graphs for seventh order, and 374 graphs for eighth order.

We use the following standard basis operators in order to facilitate the calculation of the multiple integrals containing τ-ordered products of spin operators in series expansion:

$$L_{mn}\equiv|m\rangle\langle n|,\quad m,n=1,\overline{1}, \tag{11}$$

where $m\rangle$, $|n\rangle$ are eigenstates of H_0. These operators satisfy the usual multiplication rule and the commutation relation[12] for the standard basis operators.

The spin operators can be written in terms of the standard basis operators

$$S^+=L_{1\overline{1}},$$

$$S^-=L_{\overline{1}1},$$

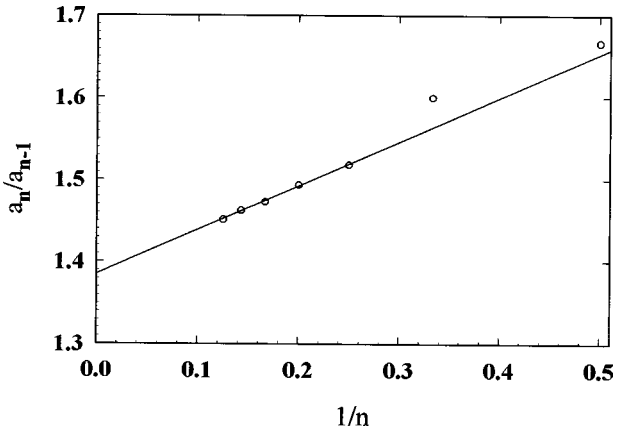

FIG. 1. The ratio of two successive coefficients of the staggered susceptibility series a_n/a_{n-1} versus $1/n$ plot for the bcc lattice.

TABLE II. Singularities $\overline{x_N}$ of the transformed staggered susceptibility series on the bcc lattice from Padé approximants to $(d/d\overline{x})\ln\chi^s(\overline{x})$ with a transformation $x=\overline{x}/(1-\overline{x}^2/4)$.

$M\backslash L$	2	3	4	5
2	0.6384	0.6484	0.6475	0.6473
3	0.6545	0.6475	0.6472	
4	0.6604	0.6473		
5	0.6429			

$$S^z=\frac{1}{2}(L_{11}-L_{\overline{11}}). \tag{12}$$

The integrals containing a product of τ-ordering operator in ΔF are calculated by using the multiple-site Wick reduction theorem and the standard basis operators.[12] The calculation of the multiple integrals containing τ-ordered products of standard basis operators is the most time consuming part of the computation. Since a large number of terms involved in the calculation are beyond the fifth order, a computer code has been developed to handle the numerous algebraic operations.

The free energy series per site F of the system is obtained as

$$F=F_0+\sum_{n=1}^{\infty} f_n(t,y)(\beta J)^n, \tag{13}$$

where f_n is a polynomial in the functions $t=\frac{1}{2}\tanh(\frac{1}{2}y)$ and $y=\beta\{JzM_0^+ + h_s\}$. We have obtained the first nine coefficients in the free energy series.

The sublattice magnetization series M^+ is calculated from the free energy series by taking a derivative with respect to h_s. Differentiating with respect to h_s, we obtain the sublattice magnetization series M^+

$$M^+=-\frac{\partial F}{\partial h_s}=\frac{\partial(\beta F)}{\partial y}=t+\sum_{n=2}^{\infty} m_n(t,t_1,y)\{\beta J\}^n, \tag{14}$$

where $t_1=dt/dy=1/(e^y+e^{-y})^2$. The polynomials of m_n for the bcc lattice are given in the Appendix. The coefficients of m_n for the sc lattice are available upon request.

The staggered susceptibility series is calculated from the sublattice magnetization series by $\chi^s=\partial M^+/\partial h_s$. After calculating the series for $\partial M^+/\partial y$, the staggered susceptibility series becomes

TABLE III. Singularities $\overline{x_N}$ of the transformed staggered susceptibility series on the sc lattice from Padé approximants to $(d/d\overline{x})\ln\chi^s(\overline{x})$ with a transformation $x=\overline{x}/(1-\overline{x}^2/4)$.

$M\backslash L$	2	3	4	5
2	0.8143	0.8380	0.8526	0.8606
3	c.c.n.	0.8673	0.8758	
4	0.8837	0.8735		
5	0.8749			

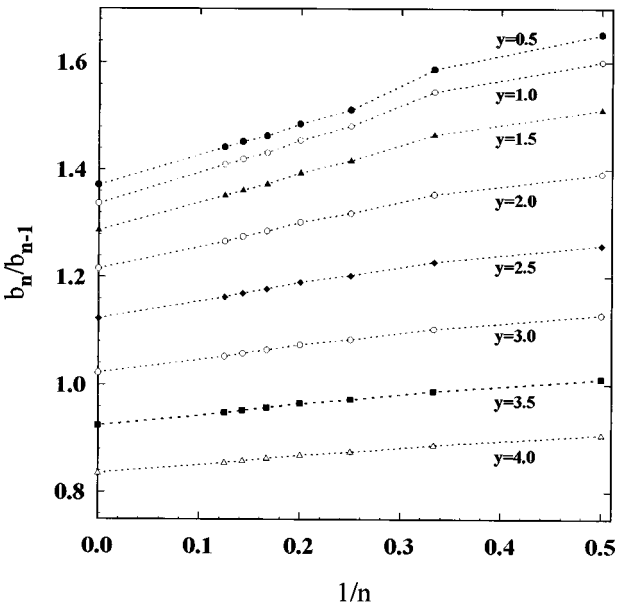

FIG. 2. The ratio of two successive coefficients of the sublattice magnetization series $\overline{M}^+$ (see text for the sublattice magnetization) b_n/b_{n-1} versus $1/n$ plot for the body-centered cubic lattice with different values of y.

$$\chi^s=\frac{\chi_c}{[1-Jz\chi_c]}, \tag{15}$$

where

$$\chi_c=\beta\frac{\partial M^+}{\partial y}. \tag{16}$$

In the disordered phase, the dimensionless zero-field ($h_s=0$) staggered susceptibility series is given as

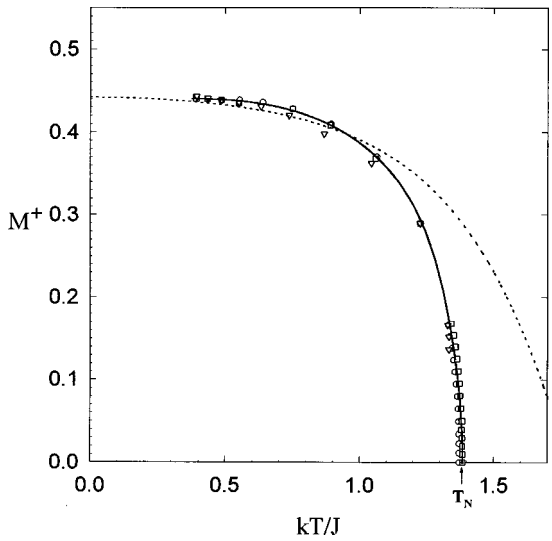

FIG. 3. The magnetic phase boundary for the bcc lattice. Solid line is the results obtained from the ratio method. The results obtained from $[\frac{3}{3}]$ (open circle), $[\frac{3}{4}]$ (square), and $[\frac{4}{3}]$ (triangle) Padé approximants are also shown. Dashed line is the predictions of spin-wave theory. T_N indicates the estimate of Néel temperature from high-temperature series.

TABLE IV. Estimates of $\bar{x}$ from the poles of Padé approximants to $[\partial \ln \bar{M}^{+}(\bar{x},y)/\partial\bar{x}]_y$ with a transformation $x=\bar{x}/(1-\bar{x}^2/9)$ for the bcc lattice.

y	$[\frac{2}{3}]$	$[\frac{2}{4}]$	$[\frac{2}{5}]$	$[\frac{3}{2}]$	$[\frac{3}{3}]$	$[\frac{3}{4}]$	$[\frac{4}{2}]$	$[\frac{4}{3}]$	$[\frac{5}{2}]$
0.5	0.6964	0.7121	0.6860	0.6959	0.6939	0.6887	0.6912	0.6827	0.6879
1.0	0.7182	0.7136	0.6628	0.7098	0.7092	0.7032	0.7091	0.7099	0.7045
2.0	0.7912	0.7759	0.7744	0.7625	0.7717	0.7734	0.7694	0.7741	0.7717
3.0	0.9009	0.9009	0.8969	0.8822	0.8927	0.8964	0.8900	0.9119	0.8935
4.0	1.0520	1.0489	1.0552	1.0368	1.0493	1.0513	1.0458	1.0699	1.0499
5.0	1.2081	1.2099	1.2156	1.1914	1.2099	1.2075	1.2036	1.2226	1.2090
6.0	1.3508	1.3591	1.3643	1.3304	1.3607	1.3763	1.3479	1.3682	1.3555
7.0	1.4743	1.4925	1.4972	1.4499	1.4991	1.4991	1.4742	1.4991	1.4845
8.0	1.5784	1.6099	1.6143	1.5504	1.6293	1.6151	1.5823	1.6136	1.5959
9.0	1.6651	1.7129	1.7169	1.6346	1.7638	1.7174	1.6741	1.7124	1.6913

$$\beta^{-1}\chi^{s}=a_0+\sum_{n=1}^{\infty} a_n\{\beta J\}^n. \tag{17}$$

In Table I we list the coefficients a_n of high-temperature staggered susceptibility series for the bcc and sc lattices.

The coefficients of our zero-field ($h_s=0$) staggered susceptibility series up to sixth order are identical to those of the high-temperature series[4,13] in the disordered phase when $M^{+}=0$. The seventh- and eighth-order graphs are checked by comparing the ferromagnetic susceptibility calculated from these graphs with the known results in the disordered phase. The susceptibility obtained from the seventh- and eighth-order graphs agree with those of the high-temperature series expansions of the spin-$\frac{1}{2}$ Heisenberg model obtained by Baker *et al.*[13,14] Furthermore we calculate the free energy and staggered susceptibility of two finite lattices by the two-point cluster method. The results of this calculation of the free energy and staggered susceptibility series agree with the series calculated by the high-temperature series expansion up to eighth order by taking $z=1$ and $p_{nx}=0$.

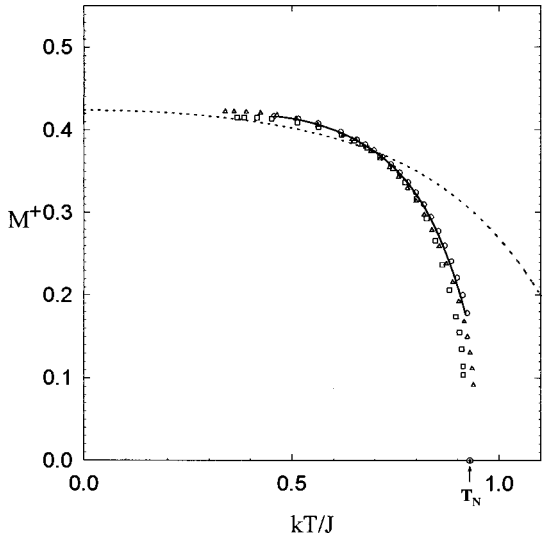

FIG. 4. The magnetic phase boundary for the sc lattice. The solid line is the results obtained from the average of the the $[\frac{2}{4}]$, $[\frac{2}{5}]$, $[\frac{3}{3}]$, and $[\frac{3}{4}]$ approximants. The results obtained from $[\frac{3}{3}]$ (open circle), $[\frac{3}{4}]$ (square), and $[\frac{4}{2}]$ (triangle) Padé approximants are also shown. The dashed line is the predictions of spin-wave theory. T_N indicates the estimate of Néel temperature from high-temperature series.

III. ANALYSIS OF THE SERIES

A. Néel temperature estimates

The staggered susceptibility series in the paramagnetic phase is given a power series expansion in the form

$$\beta^{-1}\chi^{s}=\sum_{n=0}^{\infty} a_n x^n, \tag{18}$$

where $x=J/kT$. The Néel temperature kT_N/J is estimated from the strong singularity in the paramagnetic staggered susceptibility series by using both the ratio method and Padé approximant technique. For the bcc lattice, the ratio of two successive coefficients of the staggered susceptibility series a_n/a_{n-1} versus the $1/n$ plot is shown in Fig. 1. The last five ratios lie very well on a straight line in the plot although there is very small oscillation. The Néel temperature kT_N/J is estimated from the extrapolation from the formula $kT_N/J=\mu(n,n-2)=[n\gamma_n-(n-2)\gamma_{n-2}]/2$, where $\gamma_n=a_n/a_{n-1}$. The Neville table[10,15] estimates have been constructed using $e_n^r=[ne_n^{r-1}-(n-2r)e_{n-2}^{r-2}]/2r$, where $e_n^0=a_n/a_{n-1}$. With the eighth-order series the best estimates of the last four Neville extrapolants $e_6^1[\mu(6,4)]$, $e_7^1[\mu(7,5)]$, $e_8^1[\mu(8,6)]$, and e_8^2 are 1.382, 1.384, 1.386, and 1.390, respectively. From the trend of the ratio plot, a conservative estimate for the Néel temperature is $kT_N/J=1.385\pm0.005$.

We have also used the Padé analysis of the logarithmic derivative series to estimate the Néel temperature. In the ratio plot of a_n/a_{n-1} vs $1/n$, there is a mild oscillation of the

TABLE V. A comparison of Néel temperature estimate for the bcc and sc lattices obtained from different methods.

Method	bcc	sc
Spin-wave theory (Ref. 2)	1.455	1.105
Series (Ref. 4)	1.40	0.96
Green function (Ref. 5)		0.996
Cumulant expansion (Ref. 6)	1.464	0.863
Series (present work)	1.384(5)	0.93(2)

TABLE VI. Coefficients for Eq. (A1).

n	i	$j\backslash k$	0	1	2	3	4	5	6	7	8
2	0	1		1.000							
2	1	0			−1.0000						
2	1	1	−2.0000								
2	3	1	8.0000								
3	1	1	0.3333		2.0000						
3	2	0				−2.0000					
3	3	1	−5.3333								
3	5	1	16.0000								
4	0	0				−0.0312					
4	0	1		−0.5000		−0.0625					
4	1	0			0.5000		0.1875				
4	1	1	−0.5417		3.1250						
4	2	0				−3.1250					
4	2	1		12.0000		1.5000					
4	3	0			−4.0000		−1.5000				
4	3	1	−3.8333		−26.0000						
4	4	0				13.0000					
4	4	1		−40.0000							
4	5	0			8.0000						
4	5	1	54.0000								
4	7	1	−120.0000								
5	0	0				0.2969					
5	0	1		0.0833		1.0312					
5	1	0			−0.0833		−3.0938				
5	1	1	0.4208		−0.8125		−3.5000				
5	2	0				0.8125		7.0000			
5	2	1		−5.0000		−4.5000					
5	3	0			1.6667		4.5000				
5	3	1	−8.6667		41.5000		20.0000				
5	4	0				−20.7500		−20.0000			
5	4	1		46.6667		−52.5000					
5	5	0			−9.3333		31.5000				
5	5	1	35.6000		−153.0000						
5	6	0				51.0000					
5	6	1		−112.0000							
5	7	0			16.0000						
5	7	1	21.3333								
5	9	1	−208.0000								
6	0	0				0.4941		−0.1211			
6	0	1		−0.1354		1.1471		−0.1211			
6	1	0			0.1354		−3.4414		0.6055		
6	1	1	−0.6340		4.3255		2.8594				
6	2	0				−4.3255		−5.7188			
6	2	1		−1.2500		−30.4062		−25.2656			
6	3	0			0.4167		30.4062		42.1094		
6	3	1	7.5222		8.6042		−16.5625				
6	4	0				−4.3021		16.5625			
6	4	1		86.6667		125.9375		283.7500			
6	5	0			−17.3333		−75.5625		−283.7500		
6	5	1	−112.0000		−346.6250		−49.5000				
6	6	0				115.5417		33.0000			
6	6	1		−588.0000		−84.0000					
6	7	0			84.0000		36.0000				
6	7	1	980.8889		972.0000						
6	8	0				−243.0000					

TABLE VI. (*Continued*).

n	*i*	*j**k*	0	1	2	3	4	5	6	7	8
6	8	1		1080.0000							
6	9	0			−120.0000						
6	9	1	−3586.6667								
6	11	1	4544.0000								
7	0	0				0.3242		−1.2861			
7	0	1		0.1052		−1.0026		−2.1353			
7	1	0			−0.1052		3.0078		10.6763		
7	1	1	0.4498		1.4401		20.7090		6.7930		
7	2	0				−1.4401		−41.4180		−20.3789	
7	2	1		−7.7625		49.8437		−0.5508			
7	3	0			2.5875		−49.8438		0.9180		
7	3	1	−7.8444		−17.2708		−474.8281		−246.4062		
7	4	0				8.6354		474.8281		369.6094	
7	4	1		87.8333		−319.5833		330.4297			
7	5	0			−17.5667		191.7500		−330.4297		
7	5	1	−13.5169		553.7500		2191.9688		1900.5000		
7	6	0				−184.5833		−1461.3125		−1900.5000	
7	6	1		−211.8667		−206.5000		−873.2500			
7	7	0			30.2667		88.5000		623.7500		
7	7	1	515.4540		−4063.3333		−2456.0000				
7	8	0				1015.8333		1228.0000			
7	8	1		−660.0000		3006.0000					
7	9	0			73.3333		−1002.0000				
7	9	1	−1654.6666		8130.0000						
7	10	0				−1626.0000					
7	10	1		2288.0000							
7	11	0			−208.0000						
7	11	1	−768.0000								
7	13	1	6208.0000								
8	0	0				0.4087		−0.1676		0.8311	
8	0	1		−0.1584		−0.2801		2.0886		0.5541	
8	1	0			0.1584		0.8403		−10.4431		−3.8785
8	1	1	−0.9926		1.3109		5.7298		−39.5120		
8	2	0				−1.3109		−11.4596		118.5359	
8	2	1		7.5430		50.4453		43.3770		130.9893	
8	3	0			−2.5143		−50.4453		−72.2949		−305.6416
8	3	1	17.3942		45.7361		−96.4277		265.9082		
8	4	0				−22.8681		96.4277		−398.8623	
8	4	1		−177.6086		−961.3542		−1932.6953		−1961.6699	
8	5	0			35.5217		576.8125		1932.6953		2746.3379
8	5	1	−155.0471		−119.3438		337.4219		2803.4414		
8	6	0				39.7812		−224.9479		−2803.4414	
8	6	1		2500.5556		6099.6250		13394.6093		8186.5000	
8	7	0			−357.2222		−2614.1250		−9567.5782		−8186.5000
8	7	1	76.4958		−3902.0334		−132.0417		−13062.0000		
8	8	0				975.5083		66.0208		9796.5000	
8	8	1		−16898.0000		−15193.1250		−26365.5000			
8	9	0			1877.5556		5064.3750		14647.5000		
8	9	1	9272.3193		23464.9999		−672.5000				
8	10	0				−4693.0000		269.0000			
8	10	1		51949.3333		12078.0000					
8	11	0			−4722.6667		−3294.0000				
8	11	1	−64894.0351		−36840.0001						
8	12	0				6140.0000					
8	12	1		−59072.0000							
8	13	0			4544.0000						
8	13	1	174547.3340								
8	15	1	−169111.9996								

points from a straight line. Padé approximants to the logarithmic derivative $[d \ln \chi^s(x)/dx]$ show the the presence of nonphysical singularities (complex poles) nearer to the origin than the physical singularity. In order to move the physical singularity closer the origin, we applied a conformal transformation method[10,16,17] to the series. The method rearranges the positions of the singularities and transforms the physical singularity to be nearest to the origin and isolates it from other singularities. So the transformed series represents essentially an expansion of the physical singularity.

We use the transformation[9,16]

$$x = \frac{\bar{x}}{(1-\bar{x}^2/b^2)}, \tag{19}$$

where b is a real number. Depending on the value for b, the nonphysical singularities can be mapped in different relations to the physical singularity. However, the physical singularities obtained from the d-log Padé approximant analysis of the transformed series using $b=2$ are more consistent. The Padé approximant analysis of the transformed series using $b=2$ is given in Table II. Based on Table II, a reasonable estimate for the critical point is $\bar{x}_N = 0.647 \pm 0.002$ or $x_N = 0.722 \pm 0.002$. Our best estimate of the Néel temperature for the bcc lattice is $kT_N/J = 1.384 \pm 0.005$ which is consistent with the estimate given by a ratio analysis.

We now consider the analysis of the staggered susceptibility series for the simple cubic lattice. The ratio analysis of the susceptibility series shows the irregular behavior. As in the previous case, we applied a conformal transformation method to the series. In Table III we show the d-log Padé approximant analysis of the transformed series using $b=2$. c.c.n. denotes roots of a complex pair and a negative real root rather than a positive real root. The estimate for the critical point is $\bar{x}_N = 0.87 \pm 0.01$ or $x_N = 1.07 \pm 0.02$. Based on the Padé Table II, the estimate of the Néel temperature for the sc lattice is $kT_N/J = 0.93 \pm 0.02$. We should point out that the effects of the the interference by the scattered nonphysical singularities are still present in the transformed series. Higher-order coefficients of the series for the sc lattice are needed to estimate Néel temperature more accurately.

B. The sublattice magnetization

The sublattice magnetization series of Eq. (14) is written as

$$M^+ = \sum_{n=0}^{\infty} m_n(t,t_1,y)x^n. \tag{20}$$

The sublattice magnetization M^+ is equal to zero in the disordered phase. In the ordered phase it is found self-consistently from the divergence of the series $\bar{M}$ defined as[18]

$$\bar{M}^+ = \frac{\Sigma_{n=0}^{\infty} m_n x^n}{M^+ - \Sigma_{n=0}^{\infty} m_n x^n} = \sum_{n=1}^{\infty} b_n(t,t_1,y)x^n. \tag{21}$$

If the self-consistently determined value of M^+ has been chosen then the series $\bar{M}$ diverges as the order of the series M^+ goes to infinity. It can be shown that the series of Eq. (21) reduces to the staggered susceptibility series of Eq. (18) as M^+ approaches zero, namely,

$$\lim_{M^+ \to 0} \sum_{n=1}^{\infty} b_n x^n = Jz\chi^s. \tag{22}$$

Our sublattice magnetization series obtained from Eq. (21) is identical to the staggered susceptibility series in the $M^+ = 0$ limit. This is also a check on the completeness of the sublattice magnetization as well as staggered susceptibility series. The sublattice magnetization as a function of temperature is estimated using the ratio method. For a given value of y, the series coefficients of Eq. (21) are first calculated. Then the temperature (x^{-1}) is estimated from the divergence of the series. Finally, the sublattice magnetization is calculated from $M^+ = y/xz$. The ratio of two successive coefficients of the magnetization series in the ordered phase b_n/b_{n-1} versus the $1/n$ plot for certain values of y is shown in Fig. 2. The temperature corresponding to each value of y is estimated by extrapolating the straight line to the $1/n=0$ axis. The last five ratios lie on a straight line in the plot. The presence of small oscillation suggests the use of the extrapolation formula $kT/J = \mu(n,n-2) = [n\gamma_n - (n-2)\gamma_{n-2}]/2$, where $\gamma_n = b_n/b_{n-1}$. In Fig. 3 we show the sublattice magnetization M^+ as a function of temperature T obtained from the ratio method for the bcc lattice. They are plotted as a solid line which is estimated from the average of three extrapolations $\mu(8,6)$, $\mu(7,5)$, and $\mu(6,4)$. The extrapolation shows good convergence in the sense that each extrapolation value differs from the average value by less than 1% except in the low-temperature region.

We have also performed Padé analysis on the logarithmic derivative of sublattice magnetization series of Eq. (21) with a fixed value of y. The sublattice magnetization series is transformed using the transformation of Eq. (19) in order to get better estimates of the physical singularity. For a fixed value of y, the roots of the denominators of d-log Padé approximants $([\partial \ln \bar{M}^+(\bar{x},y)/\partial \bar{x}]_y)$ to the series reflect points at which the series is singular. Table IV shows the smallest real roots of the denominator of d-log Padé approximants to the transformed series using $b=3$ for different values of y. We ignored a smaller real root which appears occasionally and coincides closely with a root of the numerator. For instance, for the $[\frac{4}{3}]$ approximant when $y=1.0$, there is a smaller root of the denominator at $\bar{x}=0.11243$, but there is the same root of the numerator at $\bar{x}=0.11243$. We note that there is agreement between different approximants in a wide range of temperatures. However, roots of the Padé approximants show oscillatory behavior in the low-temperature region.

The magnetic phase boundary M^+ vs T obtained from $[\frac{3}{3}]$, $[\frac{3}{4}]$, and $[\frac{4}{3}]$ Padé approximants is also plotted in Fig. 3. It is clear from Fig. 3 that the magnetic phase boundary estimated from the Padé approximants analysis is consistent with that obtained from the ratio analysis. The results of the $[\frac{4}{3}]$ Padé approximant shows an oscillatory behavior in the vicinity of the Néel temperature, for $0.0 < M^+ < 0.14$. The predictions of spin-wave theory[1,19] are also shown in Fig. 3 for comparison. In the low-temperature region, $kT/J < 0.4$, the convergence of the series is slow.

For the sc lattice, the ratio analysis of the sublattice magnetization series shows the irregular behavior in the vicinity of the Néel temperature where fluctuations become large. We follow the same procedure as for the bcc lattice above. We

apply the transformation of Eq. (19) to the series. The magnetic phase boundary is estimated from the transformed series with different value of the parameter b for the different Padé approximant. The optimum choice of b for the $[\frac{2}{4}]$, $[\frac{2}{5}]$, $[\frac{3}{3}]$, and $[\frac{3}{4}]$ Padé approximants is 2.0, 2.0, 3.0, and 1.0, respectively.

Compared with the Padé approximants for the bcc lattice, the Padé approximants for the sc lattice are less well converged. In Fig. 4, we show the magnetic phase boundary M^+ vs T plot for the sc lattice. In this plot the solid line is drawn through the points obtained from the average of the values given by the four successive approximants over the range $0.2<M^+<0.42$. The results of $[\frac{2}{5}]$, $[\frac{3}{3}]$, and $[\frac{3}{4}]$ Padé approximants are also plotted in Fig. 4 for comparison. The predictions of spin-wave theory[1,19] is also shown for comparison. The uncertainty in each estimate of M is the uncertainty in the estimation of temperature kT/J. The values of kT/J from different approximants near the region of the Néel temperature, for $0.0<M^+<0.2$, are not well converged for the sc lattice. A longer series is needed to locate the phase boundary with greater precision in this region.

IV. SUMMARY AND CONCLUSIONS

We have calculated the exact eighth-order linked-cluster series for the free energy, sublattice magnetization, and staggered susceptibility of the spin-$\frac{1}{2}$ Heisenberg antiferromagnet on three-dimensional bipartite lattices. In the disordered phase our staggered susceptibility series reduces to the high-temperature series. The series are analyzed by using both the ratio method and Padé approximant technique. We have used a conformal transformation method to aid in the analysis of the series. The results obtained from the analysis of the transformed series are consistent with the results given by the ratio analysis.

With the eighth-order series of the staggered susceptibility we obtain more accurate estimate of Néel temperature for the bcc lattice. For the sc lattice higher-order terms are needed to estimate the Néel temperature more accurately. A comparison of the present estimate of Néel temperature with previous estimate obtained from different methods for the bcc and sc lattices is given in Table V.

We have also shown the magnetic phase boundary for the spin-$\frac{1}{2}$ Heisenberg antiferromagnetic model for the bcc and sc lattices. A comparison with spin-wave theory in the low-temperature region is shown. For the bcc lattice, the sublattice magnetization series is well converged in a wide range of temperatures. The limiting low-temperature form of our phase boundary agrees closely with that given by the spin-wave theory. The convergence of the linked-cluster series expansion is also slow in the low-temperature region. Likewise for the sc lattice the series obtained is not well converged. However, we present the phase boundary for the sc lattice with some confidence over the range $0.2<M^+<0.4$. A longer series is needed to locate the phase boundary with greater precision.

ACKNOWLEDGMENTS

This research was supported by the National Science Council of the Republic of China under Grant No. NSC87-2112-M182-001. The computations were done on the DEC Alpha and IBM SP2 of the National Center for High-Performance Computing (NCHC). We wish to thank NCHC for its support.

APPENDIX

The coefficients of the sublattice magnetization series are polynomials in the variables t, t_1, and y as

$$m_n=\sum_{i,j,k}\beta_{ijk}^n t^i t_1^j y^{-k}. \tag{A1}$$

The coefficients in Eq. (A1) for the bcc lattice are listed in Table VI.

[1] P. W. Anderson, Phys. Rev. **86**, 694 (1952); R. Kubo, *ibid.* **87**, 568 (1952); T. Oguchi, *ibid.* **117**, 117 (1960).
[2] S. H. Liu, Phys. Rev. **142**, 267 (1966).
[3] M. G. Cottam and R. B. Stinchcombe, J. Phys. C **3**, 2283 (1970).
[4] G. S. Rushbrooke and P. J. Wood, Mol. Phys. **6**, 409 (1963).
[5] M. E. Lines, Phys. Rev. A **133**, A841 (1964); C. C. Cheng and F. C. Pu, Acta Phys. Sin. **20**, 624 (1964); B. G. Liu, Phys. Rev. B **41**, 9563 (1990); G. Z. Wei and A. Du, Phys. Solid State **175**, 237 (1993).
[6] H. Li and T. L. Chen, Phys. Rev. B **52**, 15 979 (1995).
[7] M. Wortis, in *Phase Transitions and Critical Phenomena*, edited by C. Domb and M. S. Green (Academic, New York, 1974), Vol. 3.
[8] Y. L. Wang, C. Wentworth, and B. Westwanski, Phys. Rev. B **32**, 1805 (1985); C. Wentworth and Y. L. Wang, *ibid.* **36**, 8687 (1987).
[9] K. K. Pan, Phys. Lett. A **244**, 169 (1998).
[10] D. S. Gaunt and A. J. Guttman, in *Phase Transitions and Critical Phenomena* (Ref. 7).
[11] A. A. Abrikosov, L. P. Gor'kov, and I. Ye. Dzyaloshinsky, *Quantum Field Theoretical Methods in Statistical Physics* (Pergamon, New York, 1965).
[12] K. K. Pan and Y. L. Wang, Phys. Rev. B **51**, 3610 (1995); Phys. Lett. A **178**, 325 (1993).
[13] G. S. Rushbrooke, G. A. Baker, and P. J. Wood, in *Phase Transitions and Critical Phenomena* (Ref. 7).
[14] G. A. Baker, Jr., H. E. Gilbert, J. Eve, and G. S. Rushbrooke, Phys. Rev. **164**, 800 (1967).
[15] D. Jasnow and M. Wortis, Phys. Rev. **176**, 739 (1968).
[16] D. D. Betts, C. J. Elliott, and R. V. Ditzian, Can. J. Phys. **49**, 1327 (1971).
[17] M. H. Lee and H. E. Stanley, Phys. Rev. B **4**, 1613 (1971).
[18] D. S. Gaunt and G. A. Baker, Jr., Phys. Rev. B **1**, 1184 (1970); Y. L. Wang and F. Lee, *ibid.* **29**, 5156 (1984).
[19] J. Oitmaa, C. J. Hamer, and Z. Weihong, Phys. Rev. B **50**, 3877 (1994).